PHYSICAL REVIEW B VOLUME 44, NUMBER 15 15 OCTOBER 1991-I

Inverse-photoemission spectra and electronic structure of the Cu(110) surface

J. Redinger and P. Weinberger
Institut für Technische Elektrochemie, Technische Universität Wien, A-1060 Wien, Austria

H. Erschbaumer and R. Podloucky
Institut für Physikalische Chemie, Universität Wien, A-1090 Wien, Austria

C.L. Fu* and A.J. Freeman
Department of Physics and Astronomy, Northwestern University, Evanston, Illinois 60208
(Received 2 May 1991)

We report results of a self-consistent full-potential linearized augmented-plane-wave calculation within the local-density approximation for an 11-layer slab corresponding to a Cu(110) surface. The relaxed geometry, i.e., the change of the top two interlayer spacings $\Delta_{12} = -6.2\%$ and $\Delta_{23} = +2.1\%$, was obtained by total-energy minimization. For the work function, a value of 4.84 eV was derived. Based on the self-consistent potentials of the electronic-structure calculation for the relaxed geometry, angle-resolved inverse-photoemission spectra were calculated within a one step model. Spectra were obtained for the $\overline{\Gamma}$-$\overline{X}$ and $\overline{\Gamma}$-$\overline{Y}$ symmetry lines. Two surface-related states at $\overline{X}$ and $\overline{Y}$ were found at 4.6 and 1.5 eV above the Fermi energy.

I. INTRODUCTION

The combination of a powerful first-principles method for the calculation of the electronic structure of surfaces with a first-principles theory of photoemission has been proven to yield interesting insights into the electronic structure of surfaces and to yield rather good agreement with experiment.[1,2] In the present study we focus on the angle-resolved inverse-photoemission spectra (ARIPES) for a Cu(110) surface as calculated by Pendry's time-reversed low-energy electron diffraction type method.[3] The results are based on a full-potential linearized augmented-plane-wave (FLAPW) slab calculation[4] which in turn was also used to calculate the equilibrium relaxation geometry. The Cu(110) surface is of particular interest because of the occurence of surface states and furthermore, it has been much less extensively studied than its more closely packed counterparts, Cu(001) and Cu(111). Some detailed experimental studies of the inverse photoemission spectra of Cu(110) were made by Altmann *et al.*,[5] Bartynski, Gustafsson, and Soven,[6] Reihl and Frank,[7] and Goldmann, Dose, and Borstel.[8] As regards theoretical investigations, only rather early pioneering theoretical studies of Cu(110) surface features were undertaken by Lee and Holzwarth[9] and Dempsey and Kleinman,[10] these, of course, cannot be compared with results of up-to-date electronic-structure methods. A different method for calculating the surface states was applied by Smith[11] based on a combination of elementary multiple-reflection theory and elementary nearly-free-electron theory.

II. COMPUTATIONAL DETAILS

The electronic structure and total energy of the Cu(110) surface were calculated within the local-density approximation (LDA) by the self-consistent full-potential linearized augmented-plane-wave (FLAPW) method[4] for an 11-layer slab geometry. In this calculation, the valence states were calculated semirelativistically whereas the core states were treated fully relativistically. The two-dimensional lattice parameters for the rectangular unit cell of the (110) surface were chosen to be 4.7065 and 6.656 a.u. The value of the fcc bulk lattice parameter of 6.656 a.u. was obtained by total energy minimization in a self-consistent bulk FLAPW (Ref. 12) calculation. In order to solve the eigenvalue equations the wave functions were expanded into about 450 APW functions. Potential and charge density were expanded into about 2000 star functions, with the l expansion inside the muffin-tin spheres truncated at $l_{\max} = 8$. For self-consistency, the two-dimensional Brillouin-zone integration was performed by a Gaussian smearing method using 12 inequivalent $\mathbf{k}$ points in the irreducible part of the zone.

All theoretical angle-resolved inverse-photoemission spectra (ARIPES) discussed in the present paper were calculated within the framework of the one-step theory of photoemission[3,13–16] in which a multiple-scattering technique is used for both the initial and the final states. The potential used corresponds to the muffin-tin part of the FLAPW potential, i.e., it is spherically symmetric inside the atomic spheres, constant in between, and z dependent across the surface barrier. The atomic distances and the distances between the layers are those determined in the FLAPW calculation and reflect the oscillatory relaxation of the Cu(110) surface. In particular, the muffin-tin part of the FLAPW surface potential is used in the top layer, the subsurface FLAPW potential in the next layer, and the FLAPW central potential for all other layers in the crystal. Inside the atomic spheres, the l expansion of both the high-energy and low-energy state wave functions was truncated at $l_{\max} = 4$. The high-energy states

represent incoming initial electrons and the low-energy states the additional electrons inside the (semi-infinite) crystal.

The use of 37 beams to represent the scattering between the layers turned out to be sufficient to yield converged photocurrents. The only parameters not fixed by the FLAPW calculation are the lifetimes of the electrons for the low- and high-energy states. For the ARIPES calculations they are represented by a constant imaginary contribution to the FLAPW potential. For the low-energy states the imaginary contribution was chosen to be rather small, namely -0.015 eV. For the high-energy states an energy-dependent lifetime according to McRae and Caldwell[17] was used, which amounts to -0.9 for electrons which will occupy states close to E_F, and to -2.2 eV for those electrons which will occupy states 7 eV above E_F.

The experimental geometry for collecting unpolarized photons is simulated in the present calculations by considering equal contributions of s- and p-polarized photons escaping at an angle of 45° with respect to the surface normal. Finally, after applying a Fermi-Dirac-like cutoff at E_F, the spectra are convoluted by a Gaussian spectrometer resolution function of 0.8 eV full width at half maximum. The zero of the binding energy scale is fixed at E_F.

III. ELECTRONIC STRUCTURE

From the minimization of the total energy as a function of the first two interlayer spacings we derived surface relaxations of $\Delta_{12} = -6.2\%$ and $\Delta_{23} = +2.1\%$, which are in good agreement with the experimental data.[18] The calculated work function of 4.84 eV is very close to the most recent experimental value of 4.87 eV as given by Straub and Himpsel.[19]

In Fig. 1 we show those parts of the FLAPW band structure which are relevant for the discussion of the photoelectron spectra, namely the bands along the $\overline{\Gamma}$-$\overline{Y}$ direction (corresponding to the $\Gamma XULK$ plane of the three-dimensional Brillouin zone), and along the $\overline{\Gamma}$-$\overline{X}$ direction (corresponding to the ΓXWK plane). The band structure (Fig. 1) is labeled by even (or 1) and odd (or 2) symmetry with respect to a mirror plane parallel to the corresponding directions in **k** space. In the following, we refer to states as surface states if their charge in the surface layer muffin-tin sphere is greater than 40%. For inverse photoemission, the surface states in the unoccupied energy region for $\overline{X_1}$ at 5.2 eV and for $\overline{Y_1}$ at 1.7 eV are of special importance. The contour plots in Fig. 2 show that the $\overline{Y_1}$ surface state is of p symmetry. This cut across the slab demonstrates that although most of the state is localized in the surface region, a substantial part of it is also found in the layer below; even at the central layer non-negligible contributions are observed. The rather long-range behavior of this state is due to its free-electron-like character.

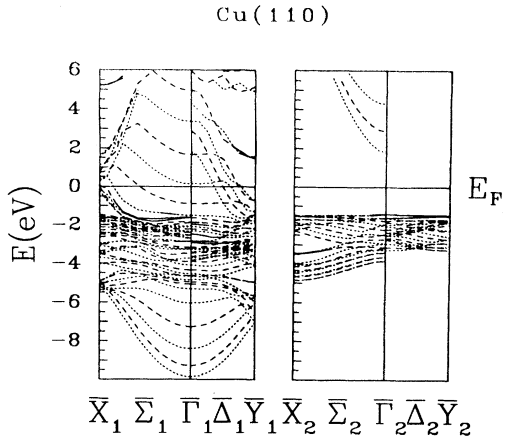

FIG. 1. Band structure for the relaxed Cu(110) surface, as obtained from an 11-layer FLAPW slab calculation. Even and odd states with respect to a mirror plane parallel to a given k direction are denoted by labels 1 and 2, respectively. Dotted and dashed lines distinguish even and odd states with respect to the central plane. Thick lines mark surface states (40% or more of the state is localized within the surface muffin-tin sphere). Energies are given with respect to the Fermi level.

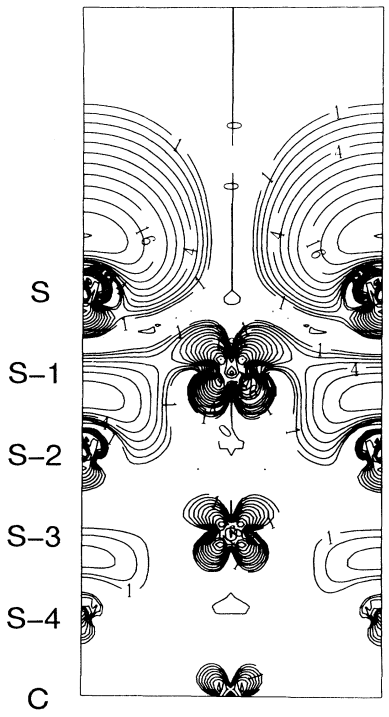

FIG. 2. Contour plot of the charge density of the $\overline{Y_1}$ surface state at 1.7 eV above the Fermi level. S denotes the surface layer, $S-1$ the layer below, etc., and C the central layer of the slab. The cut is made perpendicular to the surface along the diagonal of the rectangular two-dimensional unit cell. Units are in $0.1e/\text{a.u.}^3$.

IV. INVERSE PHOTOEMISSION

A. $\overline{\Gamma}$-$\overline{Y}$ direction

The calculated spectra along this direction are shown in Fig. 3(a). In general, two main features can be distinguished: a nondispersing shoulder close to E_F (denoted by B_1 according to Jacob *et al.*[20]), and a dispersing peak (S_1) for angles of incidence θ larger than 15°. Three sets of experimental data are available[7,20,6] which basically agree with each other and also with our calculated spectra. For easier comparison, we replotted the most recent experimental data of Jacob *et al.*[20] in Fig. 3(b).

Some discrepancies, however, concerning the relative intensities and both the binding energy and dispersion of S_1 exist between the different experimental findings. In our calculation we find the surface state S_1 at $\overline{Y}$ at 1.5 eV above E_F as compared to 1.8,[20] 2.0,[7] and 2.5 eV.[6] The calculated dispersion agrees rather well with the results of Jacob *et al.*,[20] and is also in reasonable agreement with Bartynski, Gustafsson, and Soven[6] while Reihl and Frank[7] find a substantially flatter band. Quantitatively, the dispersion expressed by the effective mass m^*/m amounts to 0.9 for our calculation, and 0.8 and 1.1 for the experiments of Jacob *et al.* and Bartynski, Gustafsson, and Soven, respectively.

The bulk-related feature B_1 between 1 eV and E_F is much more pronounced in all the experimental data than in our calculation. In the case of the surface state S_1, however, the experimental intensities are not consistent among each other. The reason for the different intensities might very well be due to light-polarization effects caused by the different experimental photon collection geometries. To shed some more light on the importance of light-polarization effects, Fig. 4 shows the contributions of the differently polarized photons to the calculated spectrum for an angle of incidence, $\theta = 35°$. According to nonrelativistic selection rules,[21] z-polarized photons ($\|\langle 110\rangle$) arise from transitions into even states with a large component of the wave function perpendicular to the surface. Low-energy states with a large component parallel to the surface, however, may generate photons either with **A** parallel or normal to the $\langle 001\rangle$ ($\overline{\Gamma}$-$\overline{Y}$) mirror plane. Hence the underlying low-energy wave functions are even or odd with respect to this mirror operation. From Fig. 4 it is immediately clear that photons polarized along the surface normal dominate the spectrum, indicating a predominant orientation of the low-energy state wave function along the surface normal, as illustrated by Fig. 2. The theoretical intensities for S_1 are consistently larger than in all three experimental sets of data. From Fig. 4, we also deduce that the peak B_1 has a significant contribution of z-polarized photons. Changing the polarization ratio in the present calculation will therefore not significantly change the ratio of intensities between B_1 and S_1, but adsorption of oxygen will reduce S_1.[22]

One has to keep in mind, however, that because of the use of the local-density approximation (LDA) our calculation corresponds to $T=0$ K. As shown by Jacob *et al.*,[20] the intensity of S_1 is strongly quenched at higher temperatures, whereas this is not the case for B_1. Ex-

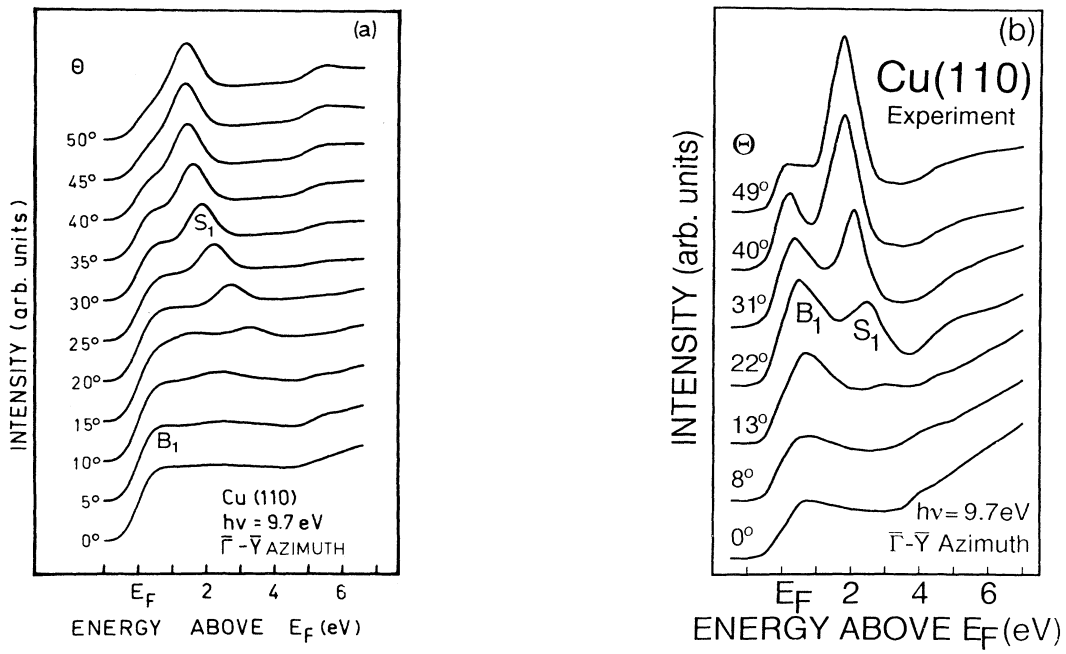

FIG. 3. Inverse-photoemission spectra for the relaxed Cu(110) surface. Electrons are incident in the $\overline{\Gamma}$–$\overline{Y}$ plane at an angle θ with respect to the surface normal. (a) Calculated spectra. (b) Experimental spectra (Ref. 20).

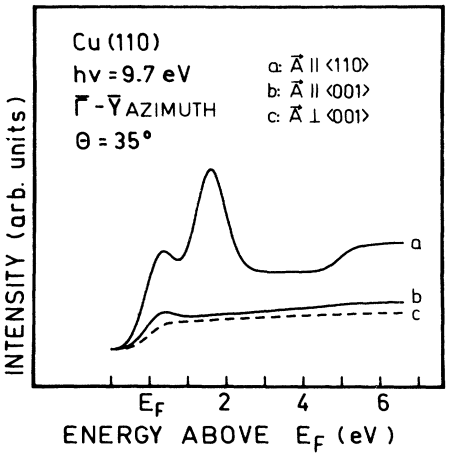

FIG. 4. Calculated inverse-photoemission spectrum for the relaxed Cu(110) surface. Electrons are incident in the $\overline{\Gamma}$-$\overline{Y}$ plane at an angle θ=35° with respect to the surface normal. (a) Photons polarized parallel to the surface normal ($\|\langle 110\rangle$). (b) Photons polarized parallel to the $\overline{\Gamma}$-$\overline{Y}$ plane ($\|\langle 001\rangle$). (c) Photons polarized perpendicular to the $\overline{\Gamma}$-$\overline{Y}$ plane ($\perp\langle 001\rangle$).

trapolating their results from room temperature down to T=0 K, we expect S_1 to dominate the spectra even more and to reduce the peak B_1 to a shoulder in accordance with our calculated result.

B. Direction $\overline{\Gamma}$-$\overline{X}$

The calculated inverse photoemission spectra along $\overline{\Gamma}$-$\overline{X}$ (ΓXWK) shown in Fig. 5(a) are characterized by two prominent peaks emerging for larger values of θ. Furthermore there is some non-negligible intensity just above E_F, which at $\theta = 22.5°$ indicates a weak peak. All three features are in good agreement with the experimental spectra,[20,23] especially with those of Jacob *et al.*[20] In order to facilitate comparison with experiment we replotted their data in Fig. 5(b). Adopting again their labeling scheme, we denote the peak just above E_F as B_1, the next-higher energy peak as B_2, and finally the third peak as S_2. It is obvious from inspection of the band structure in Fig. 1 that B_1 and B_2 are transitions into bulklike final states. S_2 corresponds to the surface-statelike band near $\overline{X}$. Strictly speaking, S_2 is found above the vacuum-zero, and represents a resonance rather than a bound state for which the wave function decays exponentially outside the crystal. However, unlike the surface resonances below the vacuum-zero, which partially couple to bulklike states, it is well located in an energy gap of the bulk crystal, just like a true surface state.

Since our ARIPES calculation is based on a multiple-scattering formalism, both boundary conditions, i.e., decaying inside the crystal and matching a scattering solution outside the crystal, are correctly fulfilled. It is quite remarkable that we find similar results also in the case of the FLAPW finite-slab model, although the underlying FLAPW basis functions are set up to vanish outside the crystal, which is certainly inappropriate for states above the vacuum-zero. This provides a strong argument in favor of a crystal-induced state, whose properties are basically determined by the crystal surface potential, and only to a lesser degree by the outside boundary conditions. As regards the energy position of S_2 we find a difference as large as −0.7 eV (i.e., the calculation is lower than experiment) at $\overline{X}$ as compared with Jacob *et al.*[20]

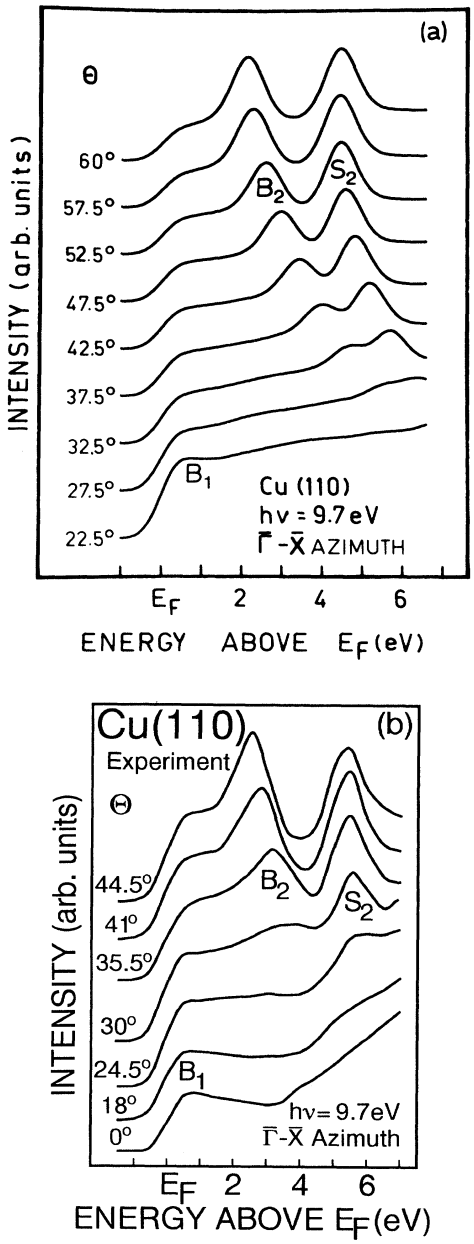

FIG. 5. Inverse-photoemission spectra for the relaxed Cu(110) surface. Electrons are incident in the $\overline{\Gamma}$-$\overline{X}$ plane at an angle θ with respect to the surface normal. (a) Calculated spectra. (b) Experimental spectra (Ref. 20).

Due to the use of the LDA, which assumes that the additional electrons are perfectly antiscreened, one would expect the theoretical peak positions to be at lower energies than the experimental ones. Furthermore, the LDA is also partly responsible for the larger dispersion of the calculated peak S_2, which causes the calculated surface-state energies to fall above the experimental ones for values of $k_{\|} < 0.95$ Å^{-1}.

Inspecting the FLAPW band structure, we find a reduced dispersion as compared to the one derived from the ARIPES calculation, and hence an apparent better agreement with experiment. Also the energy position of S_2 (5.2 eV) at $\overline{X}$ is improved. However, this improvement might be considered as fortuitous, because the outside boundary conditions of the FLAPW slab model are certainly not appropriate for states above the vacuum-zero. As the FLAPW method is based on the variational principle, we conclude that forcing an artificial decay of the wave function is equivalent to a restricted variational freedom, which causes the states to shift upwards in energy. On the other hand, the differences among the two calculated dispersions (ARIPES versus FLAPW), and the difference between the calculated ARIPES derived and the experimental dispersion might also indicate some subtle deficiencies by use of only the muffin-tin parts of the FLAPW surface potential for the ARIPES calculation. The total neglect of the lateral corrugation of the surface potential will certainly have the largest impact on surface states like S_2 which have a large probability of finding the electrons near the surface barrier.

For the bulklike states we find a similar situation, i.e., a too large dispersion of B_2 in the calculated spectra. As a consequence of the different dispersions, the experimental peak is found at a lower energy than in the calculation, at least for the values of $k_{\|}$ shown in Fig. 5(b). A crossover will occur for sufficiently large $k_{\|}$, i.e., close to $\overline{X}$. Bartynski and Gustafsson[23] published similar experimental results for $\theta < 45°$. For larger angles than 45°, i.e., close to $\overline{X}$, these authors found an additional peak at 2 eV. The bulk-derived peak of their spectrum, which corresponds to our state B_2, moves down below 1 eV at $\overline{X}$.

It is important to note, however, that there is also some discrepancy between the different experimental results. Although Jacob *et al.*[20] do not show spectra for $\theta > 44.5°$ it is obvious from Fig. 4 of their paper, and in agreement with our calculation, that they would not find a second peak even for angles larger than 44.5°. Upon extrapolating the feature B_2 in their Fig. 4 to larger $k_{\|}$, it seems that this band will become separated from the bulk-projected region. This is in agreement with the calculation of Dempsey and Kleinman,[10] who predict a second surface state at the bottom of the gap. Bartynsky and Gustafsson[23] reached a similar conclusion from a two-band model for the bulk gap around $\overline{X}$. They interpret their peak at 2 eV as a surface state or resonance. It should be noted that two crystal-induced surface states within one gap have been found[6] at $\overline{Y}$, where the lower one is already occupied.

We do not find a second low-lying surface state at $\overline{X}$ in our calculations. One might argue that the criterion used for the surface states in the FLAPW method (40% of the state localized within the surface muffin-tin sphere) might be too stringent for this more spread-out type of *s-p*-like surface state. However, also the ARIPES calculation gives no indication for such a surface state because the calculated layer contributions to the total intensity for B_2 also do not show a rapid decay as a function of the distance from the surface, as would be typical for a surface state. For a typical surface state like S_2 at $\overline{X}$, only the top two layers contribute to the total intensity. In order to analyze the problem in more detail, we show in Fig. 6 the polarization-dependent contributions of the spectrum for the angle of incidence, $\theta = 60°$. From Fig. 6 it is quite obvious that the *z*-polarized states are by far the most important ones. The in-plane states of even symmetry give a small contribution to both peaks, whereas the odd states uniformly contribute to the background. As stated above, the calculated spectra were obtained for unpolarized photons which means that photons with equal even and odd polarization are escaping at 45° with respect to the surface normal. From the findings in Fig. 6, we conclude that a variation of the mixture of polarizations will not produce additional features in the calculated spectra. Also, the relative peak heights will not be substantially changed.

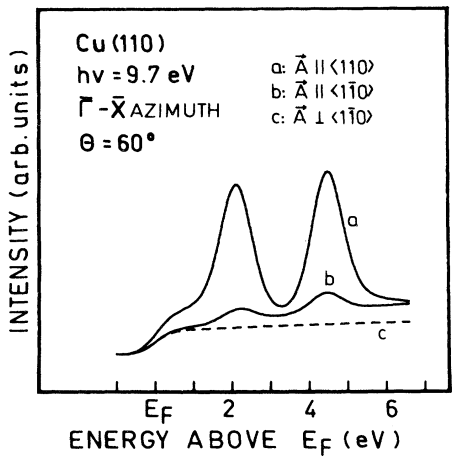

FIG. 6. Calculated inverse-photoemission spectrum for the relaxed Cu(110) surface. Electrons are incident in the $\overline{\Gamma}$–$\overline{X}$ plane at an angle θ=60° with respect to the surface normal. (a) Photons polarized parallel to the surface normal ($\|\langle 110\rangle$). (b) Photons polarized parallel to the $\overline{\Gamma}$–$\overline{X}$ plane ($\|\langle 1\bar{1}0\rangle$). (c) Photons polarized perpendicular to the $\overline{\Gamma}$–$\overline{X}$ plane ($\perp \langle 1\bar{1}0\rangle$).

V. CONCLUSION

The combination of first-principles methods such as a FLAPW model for the calculation of the surface electronic structure, and a one-step model for the calculation of ARIPES are powerful tools for a very detailed comparison to experimental spectra, concerning both peak positions and intensities. Although, for the case of Cu(110)

the agreement of measurements and calculations is rather satisfying, there remain some open interesting problems such as the possibility of a second low-lying unoccupied surface state at $\overline{X}$ which leaves interesting aspects for future studies.

ACKNOWLEDGMENTS

Work in Vienna was supported by the Austrian Fonds zur Förderung der Wissenschaftlichen Forschung (Projekt No. P7122) and by the Austrian Bundesministerium für Wissenschaft und Forschung (GZ. 49.731/2-24/91). Part of the calculations were sponsored by the EASI program at the University of Vienna Computer Center. Work at Northwestern University was supported by the U.S. National Science Foundation (Grant No. DRM88-16126) and by a computer grant from its Division for Advanced Scientific Computing at the Pittsburgh Supercomputing Center. Work at Oak Ridge National Laboratory was supported by the Division of Materials Sciences, U.S. Department of Energy, under Contract No. DE-AC05-84OR21400 with Martin Marietta Energy Systems Inc.

---

*Present address: Metals and Ceramics Division, Oak Ridge National Laboratory, Oak Ridge, TN 37831.

[1] J. Redinger, C.L. Fu, A.J. Freeman, U. König, and P. Weinberger, Phys. Rev. B **38**, 5203 (1988).
[2] U. König, P. Weinberger, J. Redinger, H. Erschbaumer, and A.J. Freeman, Phys. Rev. B **39**, 5492 (1989).
[3] J.B. Pendry, J. Phys. C **14**, 1381 (1981).
[4] E. Wimmer, H. Krakauer, and A.J. Freeman, Adv. Electron. Electron Phys. **65**, 357 (1985), and references therein.
[5] W. Altmann, V. Dose, A. Goldmann, U. Kolac, and J. Rogozik, Phys. Rev. B **29**, 3015 (1984).
[6] R. A. Bartynski, T. Gustafsson, and P. Soven, Phys. Rev. B **31**, 4745 (1985).
[7] B. Reihl and K. H. Frank, Phys. Rev. B **31**, 8282 (1985).
[8] A. Goldmann, V. Dose, and G. Borstel, Phys. Rev. B **32**, 1971 (1985).
[9] M.J.G. Lee and N.A.W. Holzwarth, Phys. Rev. B **10**, 5365 (1978).
[10] D.G. Dempsey and L. Kleinman, Phys. Rev. B **16**, 5356 (1977).
[11] N. V. Smith, Phys. Rev. B **32**, 3549 (1985).
[12] H.J.F. Jansen and A.J. Freeman, Phys. Rev. B **30**, 561 (1984).
[13] C.G. Larsson, Ph.D. thesis, Chalmers University of Technology, Gothenburg, 1982.
[14] J.B. Pendry, *Low Energy Diffraction* (Academic, New York, 1974).
[15] J.B. Pendry, Surf. Sci. **57**, 679 (1976).
[16] J.F.L. Hopkinson, J.B. Pendry, and D.J. Titterington, Comput. Phys. Commun. **19**, 69 (1980).
[17] E.G. McRae and C.W. Caldwell, Surf. Sci. **57**, 766 (1976).
[18] D.L. Adams, H.B. Nielsen, J.N. Andersen, I. Steensgard, R. Feidenhans'l, and J.E. Sørensen, Phys. Rev. Lett. **49**, 669 (1982).
[19] D. Straub and F.J. Himpsel, Phys. Rev. B **33**, 2256 (1986).
[20] W. Jacob, V. Dose, U. Kolac, and Th. Fauster, Z. Phys. B **63**, 459 (1986).
[21] J. Hermanson, Solid State Commun. **22**, 9 (1985); W. Eberhardt and F.J. Himpsel, Phys. Rev. B **21**, 5572 (1980).
[22] W. Jacob, V. Dose, and A. Goldmann, Appl. Phys. A **41**, 145 (1986).
[23] R. A. Bartynski and T. Gustafsson, Phys. Rev. B **33**, 6588 (1986).